An Investigation of Ductility Dip Cracking in Nickel-Based Filler Materials — Part I

The strain-to-fracture test has been used to develop temperature-strain relationships for ductility dip cracking

BY M. G. COLLINS AND J. C. LIPPOLD

ABSTRACT. Ductility dip cracking (DDC) is a solid-state, elevated temperature phenomenon that has been observed in thick-section, multipass austenitic stainless steel and nickel-based alloy weld metals where large grain size and high restraint are characteristic. The mechanism has been postulated to be the result of "ductility exhaustion" along the grain boundary with grain boundary sliding and the relative orientation of a grain boundary to an applied strain increasing susceptibility to DDC. Although DDC is relatively uncommon, in applications where there is low defect tolerance, its occurrence can be very costly.

In Part I of this investigation, the strain-to-fracture (STF) test, a Gleeble-based test developed by Nissley and Lippold (Ref. 1), was employed to develop STF DDC susceptibility curves for one heat of Filler Metal 52 and three heats of Filler Metal 82. Filler Metal 52 was found to be more susceptible to DDC than Filler Metal 82, with Filler Metal 82 exhibiting a heat-to-heat variation in susceptibility. Additions of hydrogen and sulfur to Filler Metal 82 were also investigated and found to increase the susceptibility of the weld metal to DDC.

Metallurgical analysis of the weld metal microstructures revealed contrasting grain boundary characteristics. Whereas Filler Metal 52 microstructures contained both straight and tortuous migrated grain boundary paths, Filler Metal 82 contained tortuous boundary paths only. Under low orders of strain and when oriented favorably to the applied load (45–90 deg), straight migrated grain boundary paths were found to be more conducive to DDC than tortuous boundary paths. Based on these grain boundary path differences, the STF test results revealing increased susceptibility to DDC for Filler Metal 52 are understood.

M. G. COLLINS and J. C. LIPPOLD are with The Ohio State University, Columbus, Ohio.

Introduction

Ductility dip cracking has been reported in a number of alloys. From a mechanistic standpoint, relatively little is known or understood about this particular type of solid-state cracking. Ductility dip cracking forms below the effective solidus temperature, and separation of grain boundaries has been reported to be characteristic of materials susceptible to DDC (Refs. 2, 3). Figure 1 schematically illustrates ductility as a function of temperature and reveals ductility dip behavior for susceptible alloys. Where thermal strains caused by manufacture or welding-induced strains intercept the ductility dip temperature range (DTR), cracking occurs.

Ductility dip cracking is often associated with the welding of heavy sections commonly encountered in critical high-pressure steam, nuclear, and power generation applications (Refs. 4–6). Although a study by Honeycombe and Gooch (Ref. 3) demonstrated that microcracking in fully austenitic weld metal is unlikely to have a detrimental effect on mechanical or fatigue properties of the weldment, DDC can have serious consequences in critical applications where defect tolerance is low and repair is both difficult and costly.

A number of factors have been reported to contribute to the development of DDC, including specific alloy, impurity and interstitial element content; solute, impurity and interstitial element segregation; grain growth; grain boundary sliding; grain boundary precipitation; grain boundary orientation relative to the applied strain; and multipass welding operations. While the DDC mechanism is not well understood, neither are the relative effects of each factor reported to contribute to the overall mechanism. Furthermore, preventive methods to avoid DDC have proven elusive.

KEY WORDS

Ductility Dip Cracking
Nickel-Based Filler Metals
Gas Tungsten Arc Welding
Strain-to-Fracture Test
Grain Boundary Characteristics
Spot Welds

This investigation addresses cracking that occurs in dissimilar welds between SA533 pressure vessel steel and Alloy 690, a nickel-based alloy that has excellent stress corrosion cracking resistance properties. Ductility dip cracking has been observed in the butter layers applied to SA533 and in the closure weld between SA533 and Alloy 690. Initially, Filler Metal 52 was used for both the butter layers and the closure weld. Cracking in Filler Metal 52 was found to be particularly severe and thus a switch to Filler Metal 82 was made. Although cracking was reduced through the application of Filler Metal 82, it was not completely eliminated.

The overall goal of this investigation was to quantify DDC susceptibility and develop a better overall understanding of the DDC mechanism in nickel-based Filler Metal 52 and Filler Metal 82. Part I quantifies DDC susceptibility in Filler Metals 52 and 82. Hydrogen and sulfur additions to the weld metal were also evaluated. Part II summarizes metallographic and fractographic studies that provided insight into the factors responsible for causing DDC while Part III uses optical microscopy, high resolution scanning electron microscopy, and electron backscattered diffraction (EBSD) techniques to further explore the factors that contribute to DDC in highly restrained Ni-base weld metals and to provide insight into the mechanism of DDC.

The STF test has proven to be a suitable, robust test technique for evaluating DDC susceptibility in weld metals. Application of this test technique successfully quantified susceptibility differences between Filler Metals 52 and 82 while also providing definitive evidence of the nega-

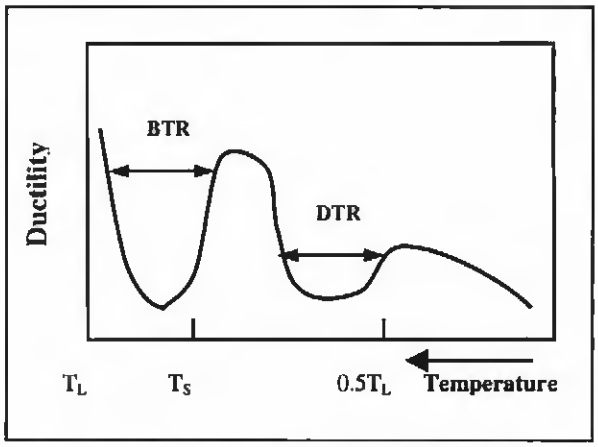

Fig. 1 — Ductility signature for a material that exhibits an elevated temperature ductility dip (BTR — Brittle Temperature Range, DTR — Ductility Dip Temperature Range).

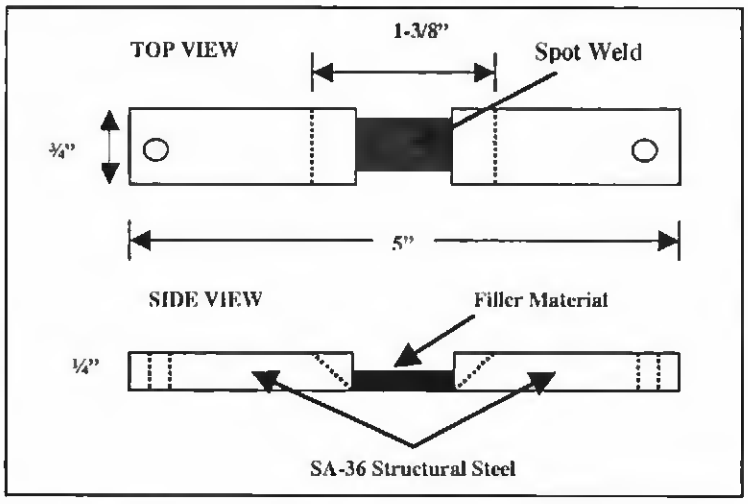

Fig. 2 — Final STF sample geometry.

tive effects on DDC susceptibility to nickel-based filler materials from additions of hydrogen and sulfur to the weld metal.

Experimental Procedure

A single heat of nickel-based Filler Metal 52 and three heats of Filler Metal 82 were evaluated in this investigation. Compositions of the respective filler metal heats are shown in Table 1. The STF test samples were produced through multiple semiautomatic gas tungsten arc welding (GTAW) cold-wire feed (CWF) stringer bead deposits into a 1¾-in.-wide × ¼-in.-deep groove machined into ¾-in.-thick SA-36 structural steel plates. As the deposited filler material was the area of interest for STF testing, low dilution of the filler material by the base material was considered critical.

The GTAW-CWF process was performed with wire feed, arc length, carriage, and voltage set control. The power source parameters were set with constant current (CC) power characteristics. Welding conditions are listed in Table 2. To avoid excessive distortion, the sample configuration extrinsic restraint was increased considerably. The increased extrinsic restraint included joining two ¾-in. SA-36 structural steel plates around their peripheries with gas metal arc welding (GMAW) and rigidly clamping the joined pieces at the corners of the joined sample plates to a welding table. Butter and fill passes were deposited in an alternately sequenced manner on opposing weld joint sides to balance distortion. In addition, stress-relieving heat treatments were periodically employed to reduce welding-induced residual stresses.

Approximately 60 weld passes were required to completely fill each of the weld grooves of the double-plate configuration (120 passes total). Once welding was completed, the GMA welds and the backside of the SA-36 structural steel plates were machined out to the bottom of the weld joint so the middle section of each STF sample would be comprised of deposited filler metal only. To facilitate both a flat surface for evaluation and to allow resistive heat concentration to the weld metal during STF testing, the sample faces were machined down approximately 1/16 in. The waterjet cutting process was utilized to remove the individual STF samples from the welded plate configuration.

After removal by the waterjet cutting process, a GTA spot weld was made within the gauge section of the samples. This spot weld was made under controlled current downslope conditions that eliminated any weld crater defects and produced a radial grain boundary pattern in the spot weld. This radial pattern favor-

Table 1 — Chemical Composition of Filler Materials (wt-%)

Element	Filler Metal 52 Heat NX9277	Filler Metal 82 Heat YN6830	Filler Metal 82 Heat YN7355	Filler Metal 82 Heat YB7724
C	0.026	0.04	0.04	0.041
Mn	0.25	2.86	2.75	2.79
Fe	8.88	1.18	0.70	0.90
S	0.0037	0.01	0.002	0.001
Si	0.17	0.12	0.07	0.06
Cu	0.011	0.09	0.07	0.04
Ni	60.12	72.75	72.8	72.98
Al	0.71	N/A	N/A	0.05
Ti	0.50	0.37	0.47	0.45
Cr	29.09	20.1	20.1	19.98
Cb + Ta	0.02	2.3	2.6	2.7
Mo	0.05	N/A	N/A	N/A
P	0.0044	0.007	0.01	0.004
Pb	0.0001	0.004	0.002	0.002
Co		0.05	0.04	0.01

Table 2 — GTAW-CWF Parameters

Welding Conditions	Butter Passes	Fill Passes
Voltage	12.5 Volts	12.5 Volts
Current	140 Amps	200 Amps
Travel Speed	2 in./min.	5 in./min.
Wire Feed Speed	5 in./min.	6 in./min.
Shielding Gas Flow (Argon)	17 ft^3/h	17 ft^3/h

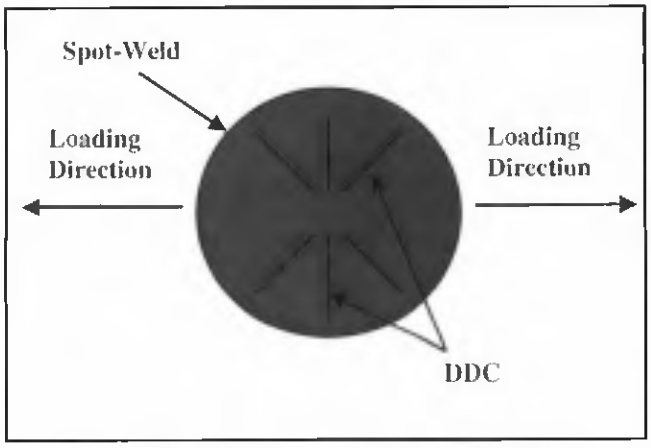

Fig. 3 — Radial pattern of DDC with respect to applied strain.

ably oriented some boundaries to the applied load and resulted in both consistent and reproducible grain boundary patterns among the STF samples. The sample faces were then lightly ground and etched to reveal the spot weld microstructure for subsequent DDC evaluation. A schematic illustration of the final STF sample is shown in Fig. 2.

Figure 3 illustrates the radial pattern of grain boundaries in the spot weld of a STF test sample. As depicted in Fig. 3, DDC typically occurred along migrated grain boundaries that were oriented at angles between 45 and 90 deg with respect to the applied loading direction.

As previously stated, the samples were tested using the Gleeble-based STF test. The samples were heated to a programmed testing temperature and held at this temperature for 10 seconds prior to stroking the Gleeble jaws at a programmed stroke rate and distance. After cooling to room temperature, the STF samples were then inspected using a binocular microscope in the 10 to 70X magnification range to determine whether or not cracks were present.

In addition to developing STF DDC susceptibility curves for Filler Metals 52 and 82, additions of hydrogen and sulfur were made to Filler Metal 82 spot welds to determine the effect of these elements on DDC susceptibility. Hydrogen was added by using 95Ar-5H_2 shielding gas. Sulfur was added to a 1/16-in.-diameter hole drilled into the middle of the STF sample gauge section. The powder was sealed into the filler metal portion of the sample by placing a small piece of 0.045-in. welding wire into the drilled hole on top of the sulfur. A low heat input, rapid spot weld was then performed to further seal in the sulfur prior to proceeding with the full spot weld cycle.

Metallographic analysis was conducted to provide insight into the nature of the grain boundaries that were susceptible to DDC. Optical microscopy samples were sectioned and mounted in phenolic powder. The samples were polished and then electrolytically etched with 10% chromic acid at 2.5 volts for approximately 15–20 seconds. During polishing, an effort was made to minimize material removal as many cracks were relatively shallow. The polished and etched samples were examined using a Nikon metallograph and pictures were taken using a Hitachi digital camera.

Results

Filler Metal 52 STF DDC Susceptibility Curves

Filler Metal 52 was tested in both the as-welded and spot-welded condition. It was anticipated that based on the grain boundary orientation differences with respect to the applied strain between the as-welded and spot-welded samples, DDC susceptibility differences would be evident. Based on the limited number of samples available, the as-welded STF samples were only tested over a temperature range of 850–1200°C. Regardless, enough samples were tested to develop an idea of the effect of grain boundary orientation with respect to the applied strain on DDC susceptibility. In the as-welded condition, Filler Metal 52 was found to have a threshold strain (E_{min}) of approximately 2.5%.

A complete STF DDC susceptibility curve was then developed for Filler Metal 52 in the spot-welded condition and is shown in Fig. 4. The DTR for Filler Metal 52 in the spot-welded condition is 625–1200°C with a threshold strain for cracking of approximately 1% at approximately 1050°C. It is interesting to note that the strain differential between no cracking and gross cracking (>3 cracks) is extremely narrow (approximately 1%) throughout the susceptible temperature range with very few samples exhibiting minor cracking (1–3 cracks).

The threshold strain to induce cracking in Filler Metal 52 varied as a function of sample condition, as-welded vs. spot-welded. Based on these observations, it is postulated that this difference is attributed to both grain boundary orientation with respect to the applied strain and the effect of multiple stress relief treatments

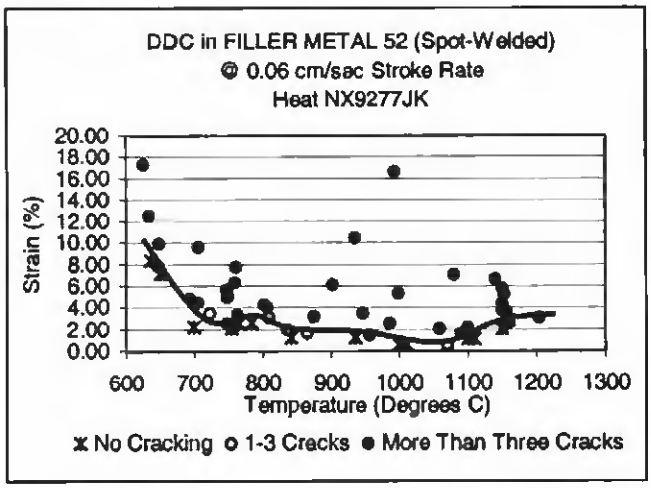

Fig. 4 — Filler Metal 52 STF DDC susceptibility curve (Heat NX9277).

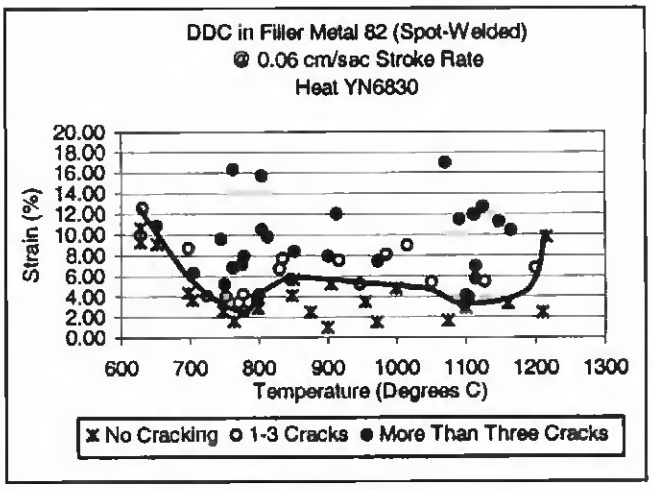

Fig. 5 — Filler Metal 82 STF DDC susceptibility curve (Heat YN6830).

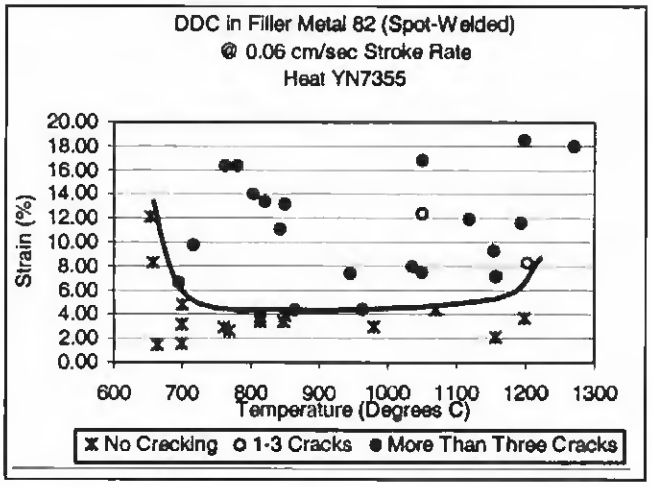

Fig. 6 — Filler Metal 82 STF DDC susceptibility curve (Heat YN7355).

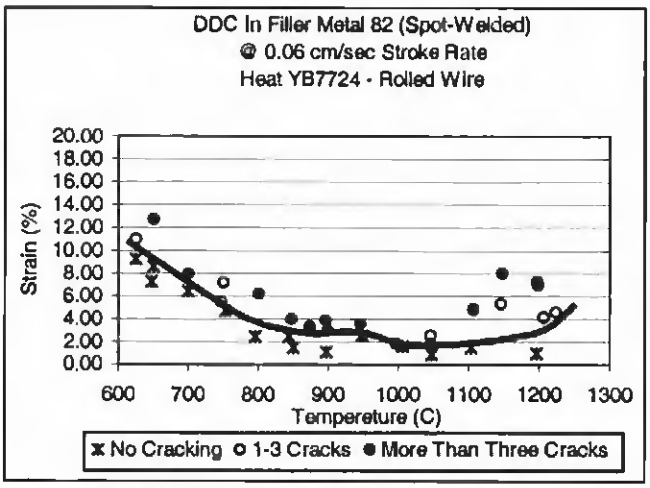

Fig. 7 — Filler Metal 82 STF DDC susceptibility curve (Heat YB7724).

of the multipass weld. The presence of grain boundaries in a radial pattern (spot-welded condition) ensures a favorable orientation for DDC, in contrast to the more random grain boundary pattern in the as-welded condition. Based on these results, all subsequent STF DDC curves were developed using spot-welded test samples.

Filler Metal 82 STF DDC Susceptibility Curves

Complete STF DDC susceptibility curves were developed for the three Filler Metal 82 heats (YN6830, YN7355, and YB7724) and are shown in Figs. 5–7, respectively. The DTR for each Filler Metal 82 heat is approximately 625–1200°C, similar to the DTR observed in Filler Metal 52. The threshold strains for YN6830, YN7355, and YB7724 are 2.5%, 4% and 1.5%, respectively.

For Filler Metal 52 (Fig. 4), the strain differential between no cracking and gross cracking (>3 cracks) is quite abrupt (approximately 1%). Conversely, the strain differential between no cracking and gross cracking in heat YN6830 of Filler Metal 82 (Fig. 5) is more gradual, on the order of 3–4%. This signifies that the strain to cause fracture is extremely sensitive for Filler Metal 52 while a quantifiable amount of strain is allowed to build up in Filler Metal 82 prior to fracture. Interestingly, as seen in Figs. 6 and 7, the same differential observed in heat YN6830 between no cracking and gross cracking is not as evident in heats YN7355 and YB7724.

Filler Metal 82 — Hydrogen Effects

A total of 16 samples from Filler Metal 82 (heat YN6830) were subjected to the STF test after hydrogen additions to a GTA spot weld utilizing a 95Ar-5H_2 shielding gas mixture. The hydrogen additions are compared to the YN6830 heat welded with 100% argon shielding in Fig. 8. Hydrogen has a pronounced negative effect on the STF characteristics of Filler Metal 82. Cracking was found to be quite significant in the 850–1000°C temperature range at applied strains of 1%. To ensure consistency, two samples each were run at 850, 950, and 1000°C, respectively. The results were strikingly similar with significant cracking observed at each temperature. As the threshold strain in this temperature range is approximately 6% when using 100% argon shielding, hydrogen additions obviously have a significant negative effect on DDC susceptibility. Furthermore, the transition from minor cracking to gross cracking (>3 cracks) occurs very abruptly in the hydrogen-containing samples, in contrast to the gradual change from minor cracking (1–3 cracks) at 6% threshold strain to significant cracking (>3 cracks) at 8% threshold strain in heat YN6830 when hydrogen was not added to the spot weld.

In addition to heat YN6830, a total of 30 samples from heat YN7355 were subjected to the STF test after similar hydrogen additions were made. These test results are compared to the YN7355 heat welded with 100% argon shielding gas in Fig. 9. Similar to heat YN6830, hydrogen has a pronounced negative effect on the STF characteristics of heat YN7355. Although the threshold strain for both heats with hydrogen additions is approximately 1%, the severity of cracking in the 850–1000°C temperature range is much greater in heat YN6830. The threshold strain for heat YN7355 is a relatively consistent 4% across the entire DTR when using 100% argon shielding gas. Hydrogen additions to heat YN7355 drop the threshold strain significantly throughout the majority of the 625–1200°C DTR. In the 850–1100°C temperature range, significant cracking (>3 cracks) was encountered in each hydrogen sample at strain levels between 2 and 4%. Furthermore, cracking was encountered all the way up to 1200°C at a strain of 1% prior to recovery of ductility at approximately 1225°C.

Filler Metal 82 — Sulfur Effects

Similar to hydrogen, additions of sulfur also increased the DDC susceptibility of Filler Metal 82, though not as dramatically. As seen in Fig. 10, sulfur additions dropped the threshold strain in the 800–1000°C temperature range from approximately 6 to 2% for heat YN6830 of Filler Metal 82. In contrast to the repeatability realized in the hydrogen samples, significant data scatter occurred with the sulfur samples. This scatter is most likely attributed to variations in the sulfur levels of the individual samples. Regardless of the exact quantity, sulfur additions resulted in negative effects to Filler Metal 82 (heat YN6830) ductility.

Metallurgical Evaluation

During this investigation, considerable metallographic analysis was performed to characterize DDC behavior of Filler Metals 52 and 82. The microstructural characteristics most prominent in both filler materials are the following:

- DDC always occurred along migrated grain boundaries
- Filler Metal 52 exhibited both straight and tortuous migrated grain boundaries
- Filler Metal 82 contained only tortuous migrated grain boundaries due to the presence of large carbides
- A majority of DDC appears to either ini-

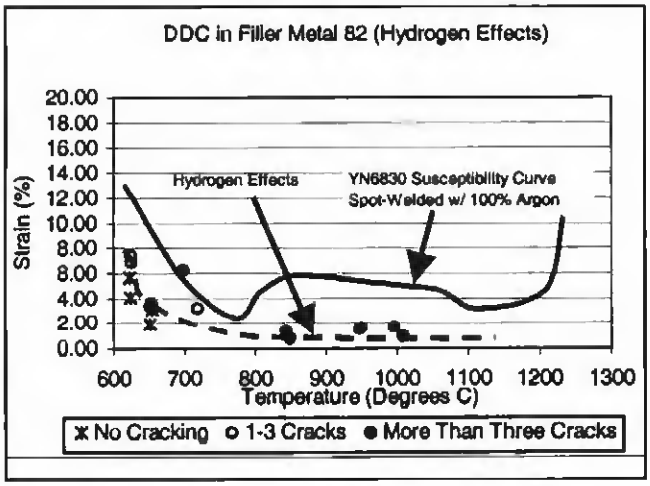

Fig. 8 — Filler Metal 82 STF DDC susceptibility curve (Heat YN6830) with hydrogen additions to the spot weld.

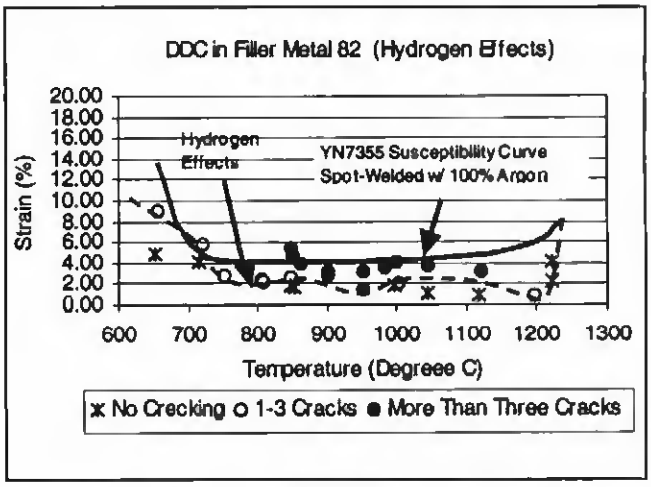

Fig. 9 — Filler Metal 82 STF DDC susceptibility curve (Heat YN7355) with hydrogen additions to the spot weld.

tiate or terminate at migrated grain boundary triple-point intersections
- Dynamic recrystallization was evident at crack tips in both filler materials in the upper temperature range (1050–1200°C) of the DTR
- Dynamic recrystallization appears to both inhibit crack initiation and suppress crack propagation, possibly signaling the onset of ductility recovery in the high-temperature range of the DTR.

Filler Metal 52. The cracks shown in Fig. 11 occur along relatively long and straight migrated grain boundaries. Note the migrated grain boundary triple-point intersections indicated by the arrows. Ductility dip cracking (DDC) appears to either initiate or terminate at these intersections possibly revealing the propensity for DDC at these high stress intensity locations. Masubuchi and Martin (Ref. 7) report effects of stress concentration at grain boundary triple-point intersections and the subsequent formation of intergranular fracture under small general deformation. Filler Metal 52 contains both straight and tortuous migrated grain boundary paths. As seen in Fig. 11, cracking is evident only along the straight sections of the migrated grain boundary.

Furthermore, note the tortuous nature of the migrated grain boundary path that is at approximately the exact orientation to the applied strain as the straight migrated grain boundaries that separated (top of Fig. 11). Under low orders of strain, the tortuous nature of the boundary appears to be a factor in its resistance to DDC. As the subject boundaries are along similar orientations with respect to the applied strain, it seems reasonable that the tortuous nature of the grain boundary path inhibits both DDC initiation and propagation.

Figure 12 illustrates DDC at a migrated grain boundary triple-point intersection. The majority of the crack extends along a relatively straight portion of the migrated grain boundary. Note the migrated grain boundary to the left of the crack. It is relatively tortuous, has barely pulled away from the solidification grain boundary, and its orientation relative to the applied strain is different from the boundary that has separated. Additionally, the migrated grain boundaries associated with the triple-point intersections are tortuous, but cracking has not propagated along these paths. Perhaps the crack initiated at the highly stressed triple-point intersection and extended along the relatively straight portion of the boundary. Conversely, the crack may have initiated along the relatively straight portion of the boundary with subsequent propagation along the tortuous portion of the boundary with final arrest at the grain boundary intersection. At a relatively low strain of 2.6%, it is possible that grain boundary tortuosity inhibited propagation and ultimately resulted in crack arrest at the boundary intersection.

Filler Metal 82. Filler Metal 82 weld metal was characterized by tortuous migrated grain boundaries, as illustrated in Fig. 13. The figure illustrates cracking along migrated grain boundaries associated with grain boundary triple-point intersections, but some "secondary" cracks between triple-point intersections that have not opened are also evident. Furthermore, orientation relative to the applied strain once again appears to play a role as all cracks are positioned in a relatively similar orientation to the applied load, especially the cracks that have opened the widest.

In Filler Metal 52, it was found that DDC typically occurred only along straight migrated grain boundaries when subjected to low applied strain levels (~2%). Straight, unimpeded migrated grain boundaries were not observed in the microstructure of Filler Metal 82, thus the tortuous boundary paths typical of Filler Metal 82 must be subjected to higher applied strains to induce DDC. Based on these observations, it is postulated that tortuous grain boundary paths are a factor in inhibiting DDC formation, especially at low levels of applied strain.

Dynamic Recrystallization. Figure 14 illustrates both DDC and dynamic recrystallization that occurs in the high temperature end (1050–1200°C) of the DTR for Filler Metal 82. Recrystallization in this temperature range was also observed in Filler Metal 52. Figure 14 illustrates both relatively narrow and wide grain boundary separations. Narrow grain boundary separation is evident at migrated grain boundary triple-point intersections with no recrystallization evident at the crack tips. Conversely, wide grain boundary separations do reveal recrystallization at the crack tips, but triple-point intersections are not as evident. Perhaps both the narrow and wide grain boundary separations originated at triple-point intersections with the wide separations more favorably oriented to the applied strain. Thus, the stress concentration at the crack tips increases along these favorably oriented boundaries, ultimately resulting in dynamic recrystallization and the onset of ductility recovery within the high-temperature region of the DTR.

Hydrogen Additions. Addition of hydrogen to Filler Metal 82 resulted in a significant increase in the degree of cracking, as shown in Fig. 15. The nature of cracking appears similar to that observed in samples that do not contain hydrogen ad-

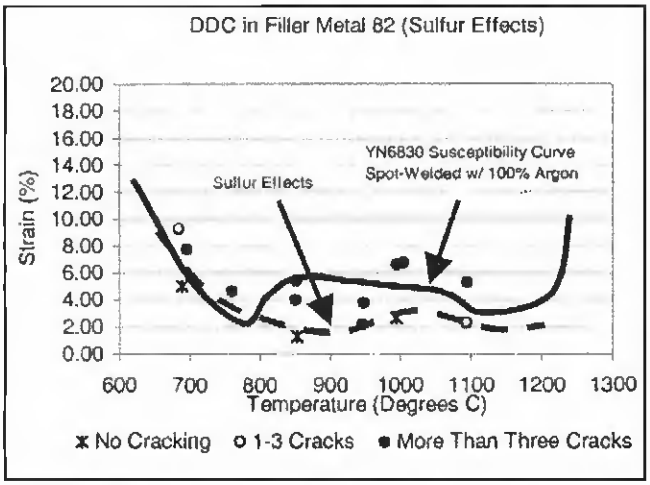

Fig. 10 — Filler Metal 82 (Heat YN6830) STF DDC susceptibility curve — effect of sulfur additions.

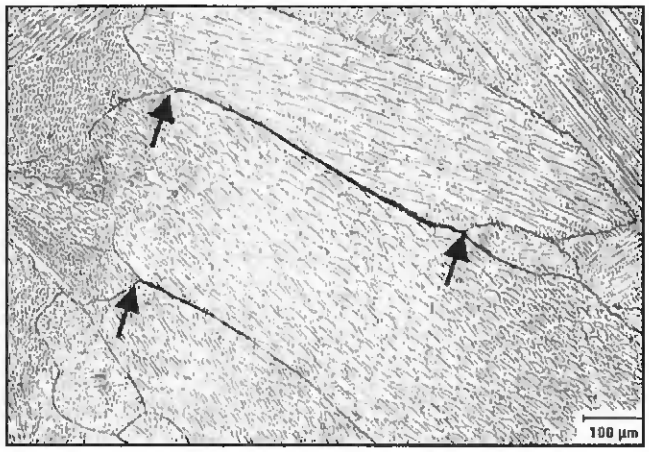

Fig. 11 — DDC along straight, migrated grain boundaries in Filler Metal 52 at 802°C and 4.4% strain (arrows indicate DDC along grain boundary triple-point intersections).

ditions, with cracks occurring along migrated grain boundaries. Additions of hydrogen simply increase the number of susceptible boundaries. A higher prevalence for cracking near triple-point grain boundary intersections was observed in these samples.

Discussion

Alloy Element Effects

Nickel-based alloys containing Nb and Ti can form both NbC and Laves phase [Ni_2(Nb,Ti)] eutectic constituents during solidification (Ref. 8). Because it contains Nb, Filler Metal 82 is capable of forming both constituents while Filler Metal 52 can only form Laves phase (Ni_2Ti). Additionally, Filler Metal 52 has a lower carbon content than all heats of Filler Metal 82, while Filler Metal 82 has lower carbon content than carbon contents reported in literature to be beneficial to ductility (Refs. 2, 9–13). It is postulated that the difference in STF DDC susceptibility behavior between Filler Metals 52 and 82 is explained by the addition of Nb and its ability to form NbC and, possibly, Laves phase eutectic constituents that inhibit grain boundary motion and contribute to grain boundary tortuosity. These constituents along the boundary also inhibit grain boundary sliding, which has been reported to be most prevalent along grain boundaries absent of such impediments (Refs. 7, 14–18). The tortuosity of the boundary can provide a mechanical locking effect that resists grain boundary sliding and subsequent cracking.

Hydrogen Effects

As shown in Figs. 8 and 9, hydrogen has a pronounced negative effect on the STF behavior of Filler Metal 82. Hydrogen cracking typically is not a concern in fully austenitic structures based on the high solubility of hydrogen and its low diffusivity in austenitic microstructures. Regardless, atomic hydrogen is an extremely mobile interstitial addition and hydrogen cracking may occur in austenitic materials if sufficient hydrogen is present. The Decohesion Theory for hydrogen cracking may help explain the increase in DDC susceptibility upon adding hydrogen to the weld pool (Refs. 19, 20). Based on this theory, hydrogen diffuses to regions of the crystal lattice where tensile stress concentrations occur. Hydrogen diffusing through a metal lattice accumulates most easily at metallurgical inhomogeneities or "traps." Perhaps at a critical temperature (~950°C) within the DTR, diffusion to the grain boundary is maximized, allowing atomic hydrogen to recombine and form molecular hydrogen (H_2) that "de-traps," subsequently decreasing grain boundary cohesion leading to intergranular fracture. Additionally, triple-point grain boundary intersections may be classified as shallow, reversible traps. These particular traps permit rapid hydrogen transport to the crack tip resulting in a critical concentration of hydrogen necessary to initiate cracking, further enhancing fracture under low orders of strain (Ref. 21).

Optical microscopy was performed to determine if, in fact, the frequency of DDC at triple-point grain boundary intersections increased when hydrogen was intentionally added to the weld metal. Based on metallographic observations, the frequency of DDC near triple-point grain boundary intersections increases when adding hydrogen to the weld metal microstructure. At relatively low levels of strain (<3%), cracking is predominant at these intersections (Fig. 15), supporting

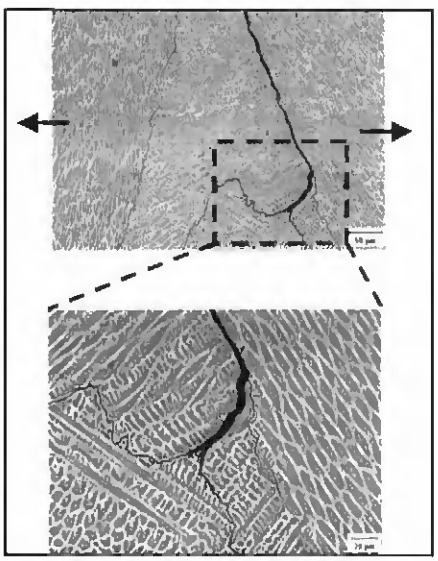

Fig. 12 — DDC along a triple-point intersection in Filler Metal 52 at 986°C and 2.6% strain (arrows indicate loading direction of the sample).

the hypothesis that hydrogen diffuses to regions of the crystal lattice where tensile stress concentrations are present, decreasing grain boundary cohesion and ultimately increasing DDC susceptibility.

Effect of Triple-Point Junctions

The presence of triple-point grain boundary intersections in polycrystalline materials has been shown to influence several material properties, including ductility, grain boundary migration, sliding, and recrystallization (Refs. 22, 23). Watanabe (Ref. 22) reported that a computer simulation study of intrinsic stress distributions at triple-point grain boundary intersections revealed that uncompensated

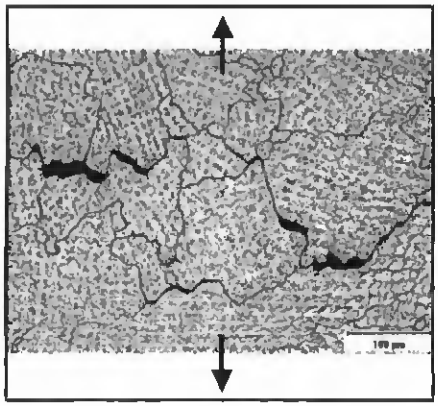

Fig. 13 — DDC along tortuous grain boundary paths in Filler Metal 82 at 972°C and 7.5% strain (arrows indicate loading direction of the sample).

stresses exist at these intersections, supporting the hypothesis that triple-point grain boundary intersections are highly stressed regions conducive to fracture initiation.

Masubuchi and Martin (Ref. 7) and Haddrill and Baker (Ref. 18) describe cracking along triple-point grain boundary intersections and attribute the cracks to a combination of increased stress concentration at the intersection and grain boundary sliding. Ductility dip cracking appears to either initiate or terminate at these intersections. It is possible that cracking initiates at these triple-point grain boundary intersections as these locations have high stress concentrations lowering the amount of stress necessary to initiate cracking. In support of this hypothesis, Fig. 12 shows a triple-point migrated grain boundary intersection. Two of the three boundaries that make up the intersection are tortuous with DDC occurring only along the relatively straight migrated grain boundary. Furthermore, Figs. 11, 13, and 15 illustrate DDC along triple-point migrated grain boundary intersections with the crack openings appearing largest at the intersections, similar to that described by the previous researchers (Refs. 7, 18). It is postulated that DDC initiated at the highly stressed triple-point intersections and extended by a grain boundary sliding mechanism along the relatively straight, low flow stress portions of the boundary that were relatively free of the eutectic constituents necessary to impede crack propagation.

Dynamic Recrystallization

A combination of mechanical work and thermal energy promotes recrystallization. High local strains at the crack tip lower the amount of thermal energy necessary to induce recrystallization. Additionally, strain concentrates along grain boundaries that have not separated. As temperature increases, recrystallization occurs more easily at these strained grain boundaries. It appears that the combination of applied strain, stress concentration at the grain boundary, high local strains at the crack tip, and applied thermal energy increases the likelihood of dynamic recrystallization. Therefore, it is possible that the onset of dynamic recrystallization within the microstructure leads to ductility recovery in the high-temperature region (1050–1200°C) of the overall DTR.

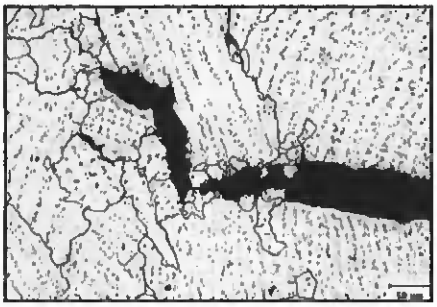

Fig. 14 — Recrystallization at crack tips in Filler Metal 82 at 1147°C and 11% strain.

Boundary Orientation Relative to the Applied Strain

It is apparent that grain boundary orientation to the applied strain is a factor in DDC formation. Previous studies by Bowers (Ref. 4) and Kikel and Parker (Ref. 6) using the double-spot varestraint test revealed an effect on DDC susceptibility from grain boundary orientation relative to the applied strain. During this investigation, STF samples were tested in both the as-welded and spot-welded condition. The as-welded condition results in a more random grain boundary pattern with epitaxial, columnar grain growth. Conversely, the spot-welded condition results in a radial grain boundary pattern, with grain boundary angles varying between 0 and 90 deg with respect to the applied strain. In the as-welded condition, a threshold strain of 2.5% was required for DDC while the spot-welded condition only required a strain of 1%.

Migrated grain boundaries in certain areas of the Filler Metal 52 microstructure decreased their energy by straightening out. Upon being subjected to a favorably oriented strain, cracking easily occurred along these straight boundaries. Interestingly, a trend developed that revealed straight migrated grain boundaries that cracked at approximately an exact orientation relative to the applied strain as tortuous migrated grain boundaries that did not crack. Based on both STF and double-spot varestraint test results, it seems reasonable to conclude that grain boundary orientation relative to the applied strain is a factor in DDC formation.

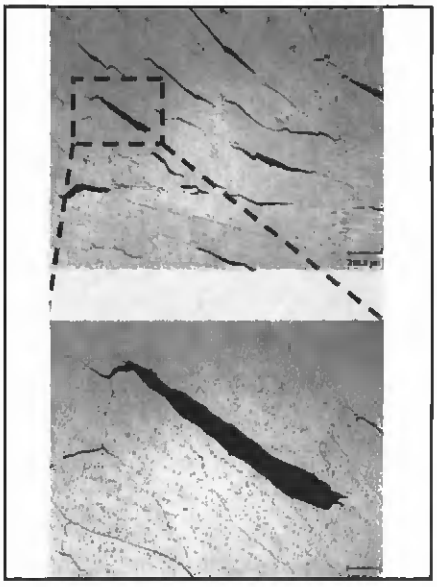

Fig. 15 — Filler Metal 82 DDC at triple-point grain boundary intersections — hydrogen additions in Filler Metal 82 at 950°C.

Conclusions

1) The DDC susceptibility of the materials tested (spot-welded condition), reported from highest to lowest susceptibility, are as follows:

- Filler Metal 52, Heat NX9277 (DTR 625–1200°C), E_{min} – 1%
- Filler Metal 82, Heat YN6830 (hydrogen additions), E_{min} – 1%
- Filler Metal 82, Heat YN7355 (hydrogen additions), E_{min} – 1%
- Filler Metal 82, Heat YN6830 (sulfur additions), E_{min} – 1.5%
- Filler Metal 82, Heat YB7724 (DTR 625–1200°C), E_{min} – 1.5%
- Filler Metal 82, Heat YN6830 (DTR 625–1200°C), E_{min} – 2.5%
- Filler Metal 82, Heat YN7355 (DTR 625–1200°C), E_{min} – 4%

2) Filler Metal 82 exhibits heat-to-heat variation in DDC susceptibility. The basis of this variation is not clear.

3) Both hydrogen and sulfur additions increase susceptibility to DDC in Filler Metal 82.

4) Straight migrated grain boundaries crack under low levels of strain (<2%). Higher strains (>2%) are necessary to initiate cracking along tortuous migrated grain boundaries.

5) Grain boundary orientation to the applied strain is a contributing factor to DDC formation.

6) Triple-point grain boundary inter-

sections provide a high stress intensity region conducive to crack initiation and/or tortuous regions conducive to crack arrest.

7) Recrystallization was observed in the upper temperatures range (1050–1200°C) of the DTR and coincided with ductility recovery.

Acknowledgments

The authors are indebted to Nathan Nissley, Antonio Ramirez, Dan Ryan, and Shu Shi, members of the Welding and Joining Metallurgy Group at The Ohio State University, for their valuable assistance during this investigation. We are grateful for the financial support from BWX Technologies, Inc.

References

1. Nissley, N. E. 2002. Development of the strain-to-fracture test to study ductility dip cracking in austenitic alloys. M.S. thesis, The Ohio State University, Columbus, Ohio.

2. Hemsworth, B., Boniszewski, T., and Eaton, N. F. 1969. Classification and definition of high temperature welding cracks in alloys. *Metal Construction and British Welding Journal* (2): 5–16.

3. Honeycombe, J., and Gooch, T. G. 1970.Microcracking in fully austenitic stainless steel weld metal. *Metal Construction and British Welding Journal* (9): 375–380.

4. Bowers, R. 1997. Unpublished research. Edison Welding Institute, Columbus, Ohio.

5. Rowe, M., Lippold, J. C., and Juhas, M. C. 1997. *Summary of ductility dip cracking — Ductility dip cracking literature review.* The Ohio State University, Columbus, Ohio.

6. Kikel, J. M., and Parker, D. M. 1998. Ductility dip cracking susceptibility of Filler Metal 52 and Alloy 690. *Trends in Welding Research*, pp. 757–762.

7. Masubuchi, K., and Martin, D. C. 1962. Mechanisms of cracking in HY-80 steel weldments. *Welding Journal* 41(8): 375-s to 384-s.

8. DuPont, J. N., Robino, C. V., and Marder, A. R. 1998. Solidification and weldability of Nb-bearing superalloys. *Welding Journal* 77(10): 417-s to 431-s.

9. Matsuda, F. 1990. Hot crack susceptibility of weld metal. *Proceedings of the 1st U.S.-Japan Symposium on Advances in Welding Metallurgy*, 19–36. Miami, Fla.: American Welding Society.

10. Arata, Y., Matsuda, F., and Katayama, S. 1977. Solidification crack susceptibility in weld metals of fully austenitic stainless steels (Report II) — Effect of ferrite, P, S, C, Si, and Mn on ductility properties of solidification brittleness. *Transactions of JWRI* 6(1): 105–117.

11. Haddrill, D. M., and Baker, R. G. 1965. Microcracking in austenitic weld metal. *British Welding Journal* 12(8): 411–419.

12. Zhang, Y., Nakagawa, H., and Matsuda, F. 1985. Weldability of Fe-36% Ni alloy (Report V) — Behaviors of grain boundary sliding and cavity formation preceding reheat hot cracking in weld metal. *Transactions of JWRI* 14(2): 119–124.

13. Mintz, B., Abu-Shosha, R., and Shaker, M. 1993. Influence of deformation induced ferrite, grain boundary sliding, and dynamic recrystallization on hot ductility of 0.1-0.75%C steels. *Materials Science and Technology* 9(10): 907–914.

14. Zhang, Y., Nakagawa, H., and Matsuda, F. 1985. Weldability of Fe-36% Ni alloy (Report VI) — Further investigation on mechanism of reheat hot cracking in weld metal. *Transactions of JWRI* 14(2).

15. Rhines, F. N., and Wray, P. J. 1961. Investigation of the intermediate temperature ductility minimum in metals. *Transactions of the ASM* 54: 117–128.

16. Bengough, G. D. 1912. A study of the properties of alloys at high temperatures. *Journal, Institute of Metals* 7: 123–174.

17. Mathew, M. D., Sasikala, G., Mannan, S. L., and Rodriguez, P. 1993. A comparative study of the creep rupture properties of Type 316 stainless steel base and weld metals. *Transactions of the ASME, Journal of Engineering Materials and Technology* 115: 163–170.

18. Haddrill, D. M., and Baker, R. G. 1965. Heat affected zone cracking in thick section austenitic steels during post weld heat treatment. *BWRA Bulletin* 6(11): 282–288.

19. Troiano, A. R. 1960. The role of hydrogen and other interstitials in the mechanical behavior of metals. *Transactions of the ASM* 52(1): 54–80.

20. Savage, W. F., Nippes, E. F., and Szekeres, E. S. 1976. Hydrogen induced cracking in a low alloy steel. *Welding Journal* 55(9): 276-s to 283-s.

21. Jones, D. A. 1996. *Principles and Prevention of Corrosion*, 2d ed. Upper Saddle River, N.J.: Prentice & Hall, Inc.

22. Watanabe, T. 1988. The potential for grain boundary design in materials development. *Materials Forum* 11: 284–300.

23. Palumbo, G., and Aust, K. T. 1992. Special properties of Σ grain boundaries. *Materials Interfaces — Atomic Level Structure and Properties*, pp. 190–211. Great Britain: Chapman-Hall.

CAN WE TALK?

The *Welding Journal* staff encourages an exchange of ideas with you, our readers. If you'd like to ask a question, share an idea or voice an opinion, you can call, write, e-mail or fax. Staff e-mail addresses are listed below, along with a guide to help you interact with the right person.

Publisher
Jeff Weber
jweber@aws.org, Extension 246
General Management,
Reprint Permission,
Copyright Issues

Editor
Andrew Cullison
cullison@aws.org, Extension 249
Article Submissions

Senior Editor
Mary Ruth Johnsen
mjohnsen@aws.org, Extension 238
Feature Articles

Associate Editor
Susan Campbell
campbell@aws.org, Extension 244
Society News
Personnel

Associate Editor
Ross Hancock
hancock@aws.org, Extension 226
New Products
New Literature

Production Editor
Zaida Chavez
zaida@aws.org, Extension 265
Design and Production

Advertising Sales Director
Rob Saltzstein
salty@aws.org, Extension 243
Advertising Sales

Advertising Production Coordinator
Frank Wilson
fwilson@aws.org; Extension 465
Advertising Production

Advertising Sales & Promotion Coordinator
Lea Garrigan
garrigan@aws.org, Extension 220
Production and Promotion

Peer Review Coordinator
Doreen Kubish
doreen@aws.org, Extension 275
Peer Review of Research Papers

Welding Journal Dept.
550 N.W. LeJeune Rd.
Miami, FL 33126
(800) 443-9353
FAX (305) 443-7404